

New Structural Motifs in Manganese Single-Molecule Magnetism from the Use of Triethanolamine Ligands**

Muralee Murugesu, Wolfgang Wernsdorfer, Khalil A. Abboud, and George Christou*

Single-molecule magnets (SMMs) are molecules with a large barrier (vs kT) to magnetization relaxation, and consequently display magnetization versus applied-field hysteresis loops at low enough temperatures, the diagnostic property of a magnet.^[1] Such molecules derive their properties from a combination of a large ground-state spin (S) value and a significant magnetoanisotropy of the Ising (easy-axis) type. SMMs thus offer a molecular approach to nanoscale magnetic materials, and their potential applications include information storage at the molecular level and use as quantum bits (qubits) in quantum computation.

Manganese carboxylate chemistry has been the main source of new SMMs during the last several years,^[2] and we are therefore seeking to develop new synthetic methodology to manganese clusters of various nuclearities and structural types. In earlier work, we showed how the tridentate (N,O,O) chelate, pyridine-2,6-dimethanol (pdmH₂) provided access to [Mn₄(O₂CMe)₂(pdmH)₆]²⁺ ions with $S = 9$,^[2b,c] [Mn₉(O₂CEt)₁₂(pdm)(pdmH)₂(L)₂] with $S = 11/2$,^[2h] and [Mn₂₅O₁₈(OH)₂(N₃)₁₂(pdm)₆(pdmH)₆]²⁺ with $S = 51/2$,^[2q] all of which are SMMs. As an extension to this work, we have recently been exploring reactions with the related molecule triethanolamine (teaH₃) to see what kind of manganese clusters might result from the use of this potentially tetradentate (N,O,O,O) chelate, which is also more flexible than pdmH₂. There are only a very few reported examples of manganese compounds obtained with teaH₃.^[3] We herein report the results of our study, which has produced new Mn₆, Mn₈, and Mn₁₆ clusters.

We have investigated many reactions between teaH₃ and a number of manganese carboxylate sources, by using different molar ratios and under a variety of conditions, and three new manganese clusters are described herein. The reaction of [Mn₃O(O₂CCHPh₂)₆(py)₃](ClO₄) (py = pyridine) with teaH₃ in a 1:2 ratio in MeCN yielded the mixed-valent (Mn^{III}₂, Mn^{II}₄) complex [Mn₆(teaH)₂(teaH₂)₂(O₂CCHPh₂)₈]₄MeCN (1·4MeCN) in 42% yield. This complex crystallizes in the triclinic $P\bar{1}$ space group. The centrosymmetric structure^[4]

[*] Dr. M. Murugesu, Dr. K. A. Abboud, Prof. Dr. G. Christou
Department of Chemistry
University of Florida
Gainesville, FL 32611-7200 (USA)
Fax: (+1) 352-392-8757
E-mail: christou@chem.ufl.edu
Dr. W. Wernsdorfer
Laboratoire Louis Neel CNRS
38042 Grenoble Cedex 9 (France)

[**] This work was supported by the National Science Foundation.

(Figure 1) contains a central planar Mn_4 rhombus (Mn1, Mn2 and their symmetry partners); each of the two doubly deprotonated $teaH^{2-}$ groups act as a tetradentate chelate to Mn1 and Mn1', and provide edge-bridging atoms O1 and O5, and capping atom O3 (and their symmetry partners); O2 is the protonated O atom. This central rhombus is very similar to that in $[Mn_4(O_2CMe)_2(pdmH)_6]^{2+}$ ^[2b,c] (and also the very similar hmp^- analogue, where hmp^- is the anion of 2-hydroxypyridine^[5]) except that the Mn^{II} and Mn^{III} sites are interchanged. A further two Mn^{II} ions (Mn3 and Mn3') in **1** are each connected to the central rhombus by two carboxylate groups and an alkoxide O atom (O8) of a singly deprotonated $teaH_2^-$ group, which is also acting as a tridentate chelate to Mn3; atoms O9 and O13 are both protonated. The Mn^{III} ions show Jahn–Teller (JT) distortions (elongations), shown as the solid black bonds in Figure 1.

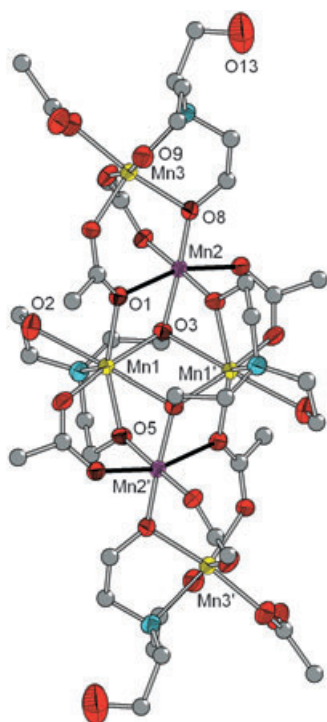


Figure 1. ORTEP representation of complex **1** with the thermal ellipsoids set at 50% probability. H atoms have been omitted for clarity. Solid black lines indicate the Mn^{III} Jahn–Teller elongation axes; Mn^{III} purple, Mn^{II} yellow, O red, N blue, C gray.

The reaction of $[Mn_{12}O_{12}(O_2CCH_2tBu)_{16}(H_2O)_4]$ with approximately 8 equivalents of $teaH_3$ in CH_2Cl_2 led to large dark brown crystals of the mixed-valent (Mn^{III}_4 , Mn^{II}_4) complex $[Mn_8(O_2CCH_2tBu)_{12}(teaH)_4] \cdot 2CH_2Cl_2$ (**2**; $2 \cdot 2CH_2Cl_2$) in 58% yield. The structure^[6] consists of an unusual Mn_8 near rectangle lying on C_2 rotation axis which passes through Mn1 and Mn5 (Figure 2). The octahedrally coordinated Mn^{II} and Mn^{III} ions alternate around the rectangle. Each Mn_2 pair is bridged by a combination of carboxylate groups and an alkoxide O atom of doubly deprotonated $teaH^{2-}$ groups; the protonated O atoms are O17 and O18. Four carboxylate groups bridge in a rare η^1, η^2, μ_3 mode, whereas the rest are in

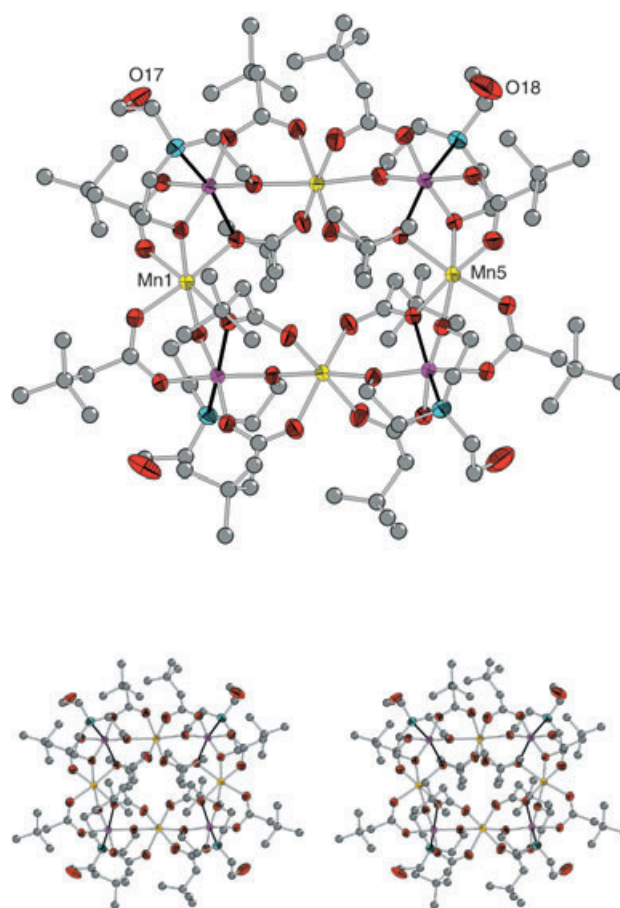


Figure 2. ORTEP representation and stereopair of complex **2** with the thermal ellipsoids set at 50% probability. H atoms have been omitted for clarity. Solid black lines indicate the Mn^{III} Jahn–Teller elongation axes. Color code as in Figure 1.

the common η^1, η^1, μ mode. The $teaH^{2-}$ groups bind as tridentate chelates to the corner (Mn^{III}) ions of the rectangle, and bridge to the adjacent Mn^{II} ions. In every case, the Mn^{III} JT elongation axes contain the $teaH^{2-}$ N atom.

The reaction between $Mn(O_2CMe)_2 \cdot 4H_2O$, $teaH_3$, and NEt_3 in a 1:1:1 ratio in MeCN led to the formation of dark brown rectangular blocks of the mixed-valent (Mn^{III}_8 , Mn^{II}_8) complex $[Mn_{16}(O_2CMe)_{16}(teaH)_{12}] \cdot 16MeCN$ (**3**; $16MeCN$) in 60% yield. The same reaction but using $NnBu_4MnO_4$ instead of NEt_3 led to same product in lower yield (30%). The structure^[7] comprises an Mn_{16} loop of alternating Mn^{II} and Mn^{III} ions with a saddle-shaped or closed sinusoidal conformation (Figure 3). Although involving a bigger loop size, the structure of **3** has similarities to that of **2**; again, eight of the mono-protonated $teaH^{2-}$ groups bind one each to the Mn^{III} ions in a tridentate chelate fashion, and bridge with their alkoxide O atoms to adjacent Mn^{II} ions; the protonated (alcohol) arms are unbound. The remaining four $teaH^{2-}$ groups bind one each to every other Mn^{II} ion around the loop in a tetradentate chelate fashion (i.e. including the protonated alcohol arm) giving seven-coordinate, distorted pentagonal-bipyramidal geometry. Each Mn_2 pair is thus again bridged by a combination of carboxylate groups and an alkoxide O atom. This is similar to the situation in Ni_{12} ^[8] and

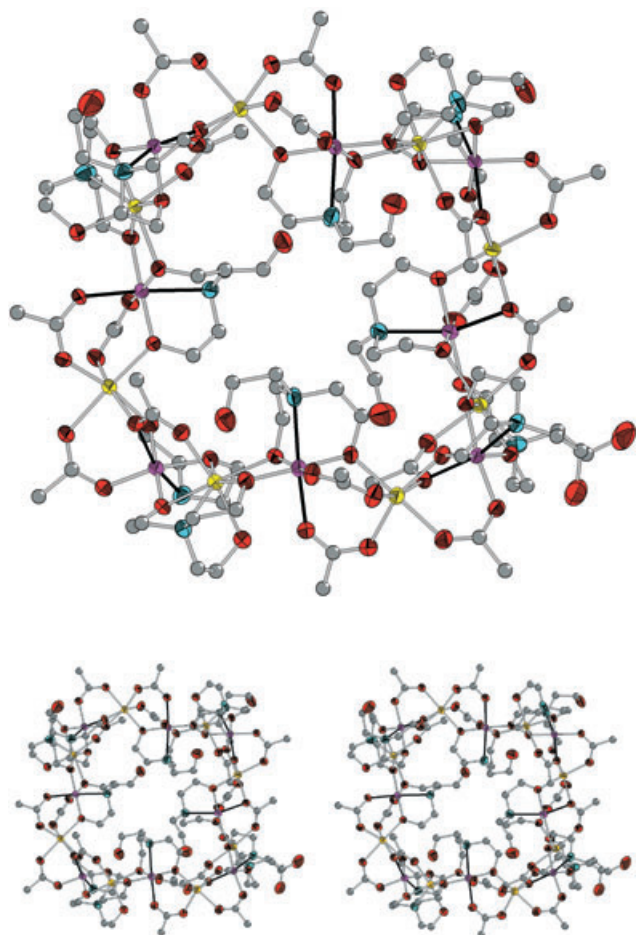


Figure 3. ORTEP representation and stereopair of complex **3** with the thermal ellipsoids set at 50% probability. H atoms have been omitted for clarity. Solid black lines indicate the Jahn–Teller axes. Color code as in Figure 1.

$\text{Fe}_{16}^{[9]}$ wheel-like complexes, the latter employing a triolate ligand. Side-views emphasizing the planar and saddle-shaped cores of **2** and **3**, are shown in Figure 4.

In all three compounds, the oxidation state assignments were made by examination of bond lengths, bond valence sum calculations, and detection of Mn^{III} JT elongation axes. JT elongated $\text{Mn}^{\text{III}}\text{--O}$ bonds for **1–3** are in the ranges 2.183(4)–2.395(6) Å (**1**), 2.182(3)–2.412(3) Å (**2**), and 2.210(2)–2.438(3) Å (**3**), significantly longer than the other $\text{Mn}^{\text{III}}\text{--O}$ bonds (1.875(4)–1.985(4) Å (**1**), 1.876(2)–1.962(3) Å (**2**), and 1.875(2)–1.979(3) Å (**3**)).

The magnetic properties of **1–3** were investigated by solid-state magnetic susceptibility (χ_M) measurements in the 5.0–300 K range in a DC field of 1000 Oe (0.1 Tesla); the resulting data are shown in Figure 5 as $\chi_M T$ vs T plots. All three compounds show a decreasing $\chi_M T$ value with decreasing temperature, which indicates that antiferromagnetic exchange interactions dominate within the molecules. The $\chi_M T$ values at 5.0 K are 10.1 (for **1**), 4.0 (**2**), and 41.4 $\text{cm}^3 \text{K mol}^{-1}$ (**3**); this suggests the complexes all have non-zero ground-state spin (S) values, with that for **3** being particularly large. To determine the ground-state S values, magnetization (M) measurements were carried out in the 1.8–

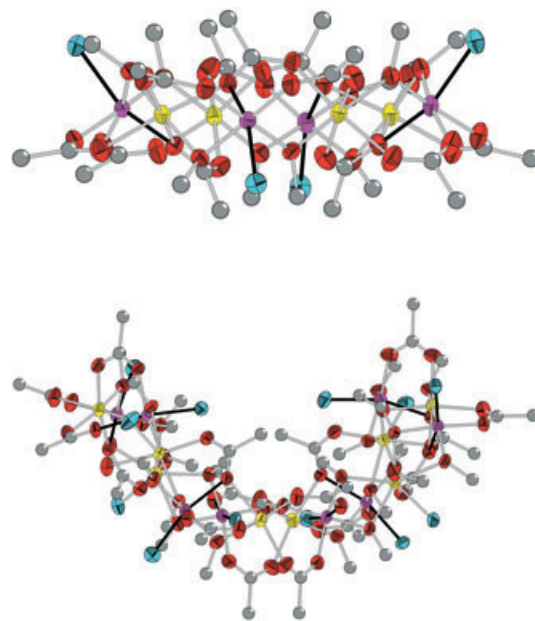


Figure 4. Side views of complexes **2** (top) and **3** (bottom) emphasizing the different conformations. Color code as in Figure 1.

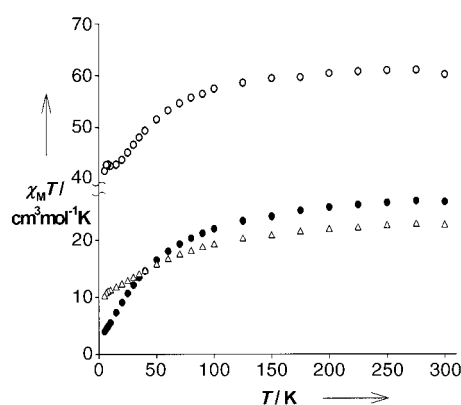


Figure 5. Plot of $\chi_M T$ versus T for complexes **1** (Δ), **2** (\bullet), and **3** (\circ).

4 K temperature and 0.1–3 T field ranges. Only low fields were used to try to avoid problems with low-lying excited states, which are expected for high-nuclearity clusters with a high density of spin states and/or when Mn^{II} ions are present, which give weak exchange interactions. We have described such problems in detail elsewhere.^[2d,r] The data were fitted by a matrix-diagonalization method to a model that assumes only the ground state is populated, includes axial zero-field splitting ($D\hat{S}_z^2$), and performs a full powder average.^[2c] Good fits were obtained for **1** with $S=5$, $g=1.79(1)$, $D=-0.20(1) \text{ cm}^{-1}$, and for **3** with $S=10$, $g=2.00(1)$, $D=-0.060(4) \text{ cm}^{-1}$. No acceptable fit for **2** could be obtained; however, its low $\chi_M T$ value (Figure 4) suggests a small ground-state spin, of $S=3$ or less.

As described elsewhere,^[2d,r] more reliable conclusions about the S value can be reached by AC magnetic susceptibility measurements, which also can detect the slow magnetization relaxation suggestive of SMMs. For **1** and **3**, fre-

quency-dependent tails were observed below approximately 3 K in the out-of-phase AC susceptibility (χ_M'') versus T signal, the maxima of which lie below the temperature limit of our SQUID instrument (1.8 K), but no tail was seen for **2**. Corresponding frequency-dependent decreases in the in-phase AC susceptibility (χ_M'), plotted as (χ_M'/T vs T), were observed for **1** and **3**, but not for **2** (Figure 6). In addition, the

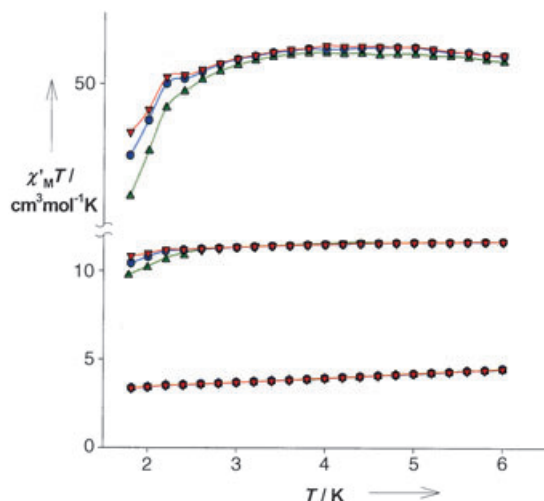


Figure 6. In-phase AC susceptibility signals (χ_M' , plotted as χ_M'/T vs T) at 1000 (\blacktriangle), 250 (\bullet) and 50 (\blacktriangledown) Hz for **1** (middle), **2** (bottom), and **3** (top).

χ_M'/T versus T plots change with temperature, confirming the presence of low-lying excited states, and extrapolation of the plots to 0 K (from regions not affected by the decreases arising from slow relaxation) gives values of approximately 11 (for **1**), 3 (**2**), and 49 $\text{cm}^3 \text{K mol}^{-1}$ (**3**). These are consistent with the values expected for $S=5$, 2, and 10, respectively, and $g=2.0$ or slightly below (as expected for Mn^{III}). The AC data thus confirm the ground-state S values deduced from the magnetization fits for **1** and **3**. In addition, the $S=2$ value for **2** is consistent with antiferromagnetic interactions between adjacent Mn^{II} and Mn^{III} ions around the ring, which would give a predicted $S=8-6=2$ ground state.

Complexes **1** and **3** were confirmed to be SMMs by magnetization versus DC-field scans on single crystals using an array of micro-SQUIDs.^[10] These gave hysteresis loops, the diagnostic behavior of magnets, below 0.5 K for **1** and 0.8 K for **3** (Figure 7), whose coercivities increase with decreasing temperature, as expected for SMMs. Further, the loops of **1** show the steps characteristic of quantum tunneling of magnetization (QTM), whereas those of **3** do not, as is usually the case for larger SMMs since they are more susceptible to step-broadening effects from low-lying excited states, intermolecular interactions, and distributions of local environments owing to ligand and solvent disorder.^[28p,q]

In summary, the use of teaH_3 has provided a useful route to three new structural types in mixed-valent manganese cluster chemistry, which include near-rectangular and closed-sinusoidal (saddle-shaped) topologies. Further, two of these complexes are also new SMMs. Complexes **2** and **3** are the

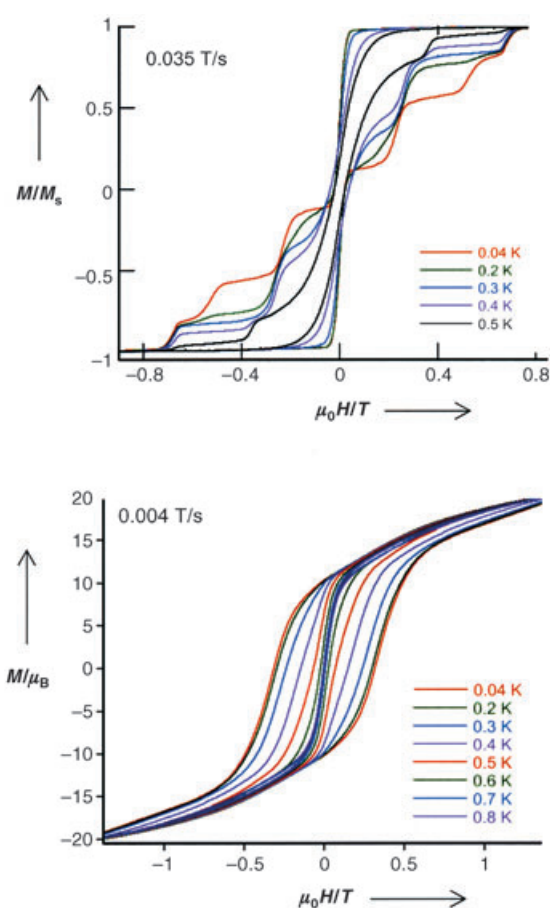


Figure 7. Magnetization (M) versus field ($\mu_0 H$ in tesla) hysteresis loops for single crystals of **1**·4 MeCN (top) and **3**·16 MeCN (bottom) at the indicated temperatures. For **1**·4 MeCN, M is normalized to its saturation value, M_s . For **3**·16 MeCN, the M value per molecule (M/μ_B) was determined from quantitative measurements.

first examples of mixed-valent Mn wheels, with **3** also being the largest single-stranded manganese loop known to date; the recently reported Mn_{22} is not a single-stranded loop.^[2p] The Mn_{16} complex **3** joins the Ni_{12} complex $[\text{Ni}_{12}(\text{chp})_{12}(\text{O}_2\text{CMe})_{12}(\text{thf})_6(\text{H}_2\text{O})_6]$ ($\text{chp}^- = 6\text{-chloro-2-pyridonate}$)^[8] and $[\text{Mn}_{12}(\text{O}_2\text{CMe})_{14}(\text{mda})_8]$ ($\text{mda}^{2-} = \text{N-methyldiethanolamine}$)^[1a] as the only single-stranded wheel/loop SMMs known to date. This is despite the relatively frequent occurrence of this structural topology.^[11] Finally, the present results illustrate once again the versatility and aesthetic beauty of manganese carboxylate chemistry.

Experimental Section

1: A solution of teaH_3 (0.075 g, 0.5 mmol) in MeCN (5 mL) was added to a stirred solution of $[\text{Mn}_3\text{O}(\text{O}_2\text{CPh}_2)_6(\text{py})_3](\text{ClO}_4)$ (0.27 g, 0.25 mmol) in MeCN (35 mL). The resultant dark brown solution was stirred for a further 15 min, filtered, and the filtrate left undisturbed at ambient temperature. After two weeks, X-ray quality brown crystals had formed and were collected by filtration, washed with MeCN, and dried in vacuo. Yield, 42%. The crystallographic sample was maintained in contact with mother liquor to prevent solvent loss and identified crystallographically as **1**·4 MeCN. Elemental analysis (%) calcd for **1**·4 MeCN: C 62.38, H 5.52, N 4.04; found: C

62.01, H 5.54, N 3.82. Selected IR data (KBr): $\nu = 3427$ (br), 2889 (br), 1575 (m), 1497 (s), 1451 (s), 1386 (m), 1068 (s), 1032 (s), 899 (s), 743 (s), 702 (m), 664 cm^{-1} (w).

2: A solution of teaH_3 (0.075 g, 0.5 mmol) in CH_2Cl_2 (10 mL) was added to a stirred solution of $[\text{Mn}_{12}\text{O}_{12}(\text{O}_2\text{CCH}_2\text{tBu})_{16}(\text{H}_2\text{O})_4]$ (0.17 g, 0.06 mmol) in CH_2Cl_2 (35 mL). The resultant dark brown solution was stirred for a further 15 min, filtered, and the filtrate left undisturbed at ambient temperature. After one week, X-ray quality dark brown crystals had formed and were collected by filtration, washed with CH_2Cl_2 , and dried in vacuo. Yield, 58%. The crystallographic sample was maintained in contact with mother liquor to prevent solvent loss and identified crystallographically as $2 \cdot 2\text{CH}_2\text{Cl}_2$. Elemental analysis (%) calcd for $2 \cdot \text{CH}_2\text{Cl}_2$: C 46.70, H 7.51, N 2.25; found: C 46.63, H 7.60, N 2.27. Selected IR data (KBr): $\nu = 3446$ (br), 2953 (s), 2866 (m), 1615 (s), 1585 (s), 1383 (s), 1297 (m), 1236 (w), 1089 (m), 910 (w), 897 (w), 730 (w), 593 cm^{-1} (m).

3: A solution of NEt_3 (0.075 mL, 0.5 mmol) in MeCN (5 mL) was added to a stirred, pale yellow-brown solution of $\text{Mn}(\text{O}_2\text{CMe})_2 \cdot 4\text{H}_2\text{O}$ (0.123 g, 0.5 mmol) and teaH_3 (0.075 g, 0.5 mmol) in MeCN (35 mL). The resulting dark brown solution was stirred for a further 15 min, filtered, and the filtrate left undisturbed at ambient temperature. After two days, X-ray quality dark brown crystals had formed and were collected by filtration, washed with MeCN, and dried in vacuo. Yield, 60%. The crystallographic sample was maintained in contact with mother liquor to prevent solvent loss and identified crystallographically as $3 \cdot 16\text{MeCN}$. Dried material is hygroscopic, and analyzed as $3 \cdot 6\text{H}_2\text{O}$. Elemental analysis (%) calcd for $3 \cdot 6\text{H}_2\text{O}$: C 33.78, H 5.88, N 4.54; found: C 33.72, H 5.80, N 4.44. Selected IR data (KBr): $\nu = 3410$ (br), 2850 (b), 1575 (m), 1409 (m), 1339(w), 1085 (m), 1036 (m), 903 (m), 746 (w), 662 (m), 572 cm^{-1} (s).

Received: August 18, 2004

Published online: December 28, 2004

Keywords: cluster compounds · magnetic properties · manganese · N, O ligands · single-molecule magnets

- [1] a) D. Foguet-Albiol, T. A. O'Brien, W. Wernsdorfer, B. Moulton, M. J. Zaworotko, K. A. Abboud, G. Christou, *Angew. Chem.* **2005**, *117*, 919; *Angew. Chem. Int. Ed.* **2005**, *44*, 897; b) A. J. Tasiopoulos, W. Wernsdorfer, K. A. Abboud, G. Christou, *Angew. Chem.* **2004**, *116*, 6498; *Angew. Chem. Int. Ed.* **2004**, *43*, 6338; c) R. Sessoli, H.-L. Tsai, A. R. Schake, S. Wang, J. B. Vincent, K. Folting, D. Gatteschi, G. Christou, D. N. Hendrickson, *J. Am. Chem. Soc.* **1993**, *115*, 1804; d) R. Sessoli, D. Gatteschi, A. Caneschi, M. A. Novak, *Nature* **1993**, *365*, 141.
- [2] a) R. Sessoli, H. Tsai, A. R. Schake, S. Wang, J. B. Vincent, K. Folting, D. Gatteschi, G. Christou, D. N. Hendrickson, *J. Am. Chem. Soc.* **1993**, *115*, 1804; b) E. K. Brechin, J. Yoo, M. Nakano, J. C. Huffman, D. N. Hendrickson, G. Christou, *Chem. Commun.* **1999**, 783; c) J. Yoo, E. K. Brechin, A. Yamaguchi, M. Nakano, J. C. Huffman, A. L. Maniero, L.-C. Brunel, K. Awaga, H. Ishimoto, G. Christou, D. N. Hendrickson, *Inorg. Chem.* **2000**, *39*, 3615; d) M. Soler, W. Wernsdorfer, K. Folting, M. Pink, G. Christou, *J. Am. Chem. Soc.* **2004**, *126*, 2156; e) W. Wernsdorfer, N. Aliaga-Alcalde, D. N. Hendrickson, G. Christou, *Nature* **2002**, *416*, 406; f) D. Price, S. Batten, B. Moubarak, K. Murray, *Chem. Commun.* **2002**, 762; g) E. Brechin, C. Boskovic, W. Wernsdorfer, J. Yoo, A. Yamaguchi, C. Sanudo, T. Concolino, A. Rheingold, H. Ishimoto, D. Hendrickson, G. Christou, *J. Am. Chem. Soc.* **2002**, *124*, 9710; h) C. Boskovic, W. Wernsdorfer, K. Folting, J. C. Huffman, D. N. Hendrickson, G. Christou, *Inorg. Chem.* **2002**, *41*, 5107; i) N. E. Chakov, K. A. Abboud, L. N. Zakharov, A. L. Rheingold, D. N. Hendrickson, G. Christou, *Polyhedron* **2003**, *22*, 1759; j) J. T. Brockman, K. A. Abboud, D. N. Hendrickson, G. Christou, *Polyhedron* **2003**, *22*, 1765; k) M. Soler, W. Wernsdorfer, K. A. Abboud, J. C. Huffman, E. R. Davidson, D. N. Hendrickson, G. Christou, *J. Am. Chem. Soc.* **2003**, *125*, 3576; l) M. Soler, W. Wernsdorfer, K. A. Abboud, D. N. Hendrickson, G. Christou, *Polyhedron* **2003**, *22*, 1777; m) A. Morello, O. N. Bakharev, H. B. Brom, L. J. de Jongh, *Polyhedron* **2003**, *22*, 1745; n) E. Brechin, M. Soler, G. Christou, M. Helliwell, S. Teat, W. Wernsdorfer, *Chem. Commun.* **2003**, 1276; o) C. J. Milios, C. P. Raptopoulou, A. Terzis, F. Lloret, R. Vicente, S. P. Perlepes, A. Escuer, *Angew. Chem.* **2004**, *116*, 212; *Angew. Chem. Int. Ed.* **2004**, *43*, 210; p) M. Murugesu, J. Raftery, W. Wernsdorfer, G. Christou, E. K. Brechin, *Inorg. Chem.* **2004**, *43*, 4203; q) M. Murugesu, M. Habrych, W. Wernsdorfer, K. A. Abboud, G. Christou, *J. Am. Chem. Soc.* **2004**, *126*, 4766; r) E. C. Sañudo, W. Wernsdorfer, K. A. Abboud, G. Christou, *Inorg. Chem.* **2004**, *43*, 4137–4144.
- [3] a) B. Pilawa, M. Keleman, S. Wanka, A. Geisselmann, A. Barra, *Europhys. Lett.* **1998**, *43*, 7; b) L. Wittick, K. Murray, B. Moubarak, S. Batten, L. Spiccia, K. Berry, *Dalton Trans.* **2004**, 1003.
- [4] a) Crystal structure data for $1 \cdot 4\text{MeCN}$: $\text{C}_{144}\text{H}_{154}\text{Mn}_6\text{N}_8\text{O}_{28}$, $M_r = 2774.39$, triclinic, space group $P\bar{1}$, $a = 14.7173(9)$, $b = 14.8251(9)$, $c = 17.6759(11)$ Å, $\alpha = 90.389(2)$, $\beta = 109.950(2)$, $\gamma = 108.101(2)^\circ$, $V = 3418.2(4)$ Å³, $T = 173$ K, $Z = 1$, 25 657 reflections collected, 11 970 unique ($R_{\text{int}} = 0.0773$), $R1 = 0.0952$, $wR2 = 0.1414$, using 8832 reflections with $I > 2\sigma(I)$. The asymmetric unit consists of half the Mn_6 and 2 MeCN molecules. b) CCDC-225868, CCDC-247748, and CCDC-225869 contain the supplementary crystallographic data for this paper. These data can be obtained free of charge via www.ccdc.cam.ac.uk/conts/retrieving.html (or from the Cambridge Crystallographic Data Centre, 12, Union Road, Cambridge CB21EZ, UK; fax: (+44)1223-336-033; or deposit@ccdc.cam.ac.uk).
- [5] J. Yoo, A. Yamaguchi, M. Nakano, J. Krzystek, W. Streib, L. Brunel, H. Ishimoto, G. Christou, D. Hendrickson, *Inorg. Chem.* **2001**, *40*, 4604.
- [6] Crystal structure data for $2 \cdot 2\text{CH}_2\text{Cl}_2$: $\text{C}_{98}\text{H}_{188}\text{Cl}_4\text{Mn}_8\text{N}_4\text{O}_{36}$, $M_r = 2579.8$, monoclinic, space group $C2/c$, $a = 26.2251(14)$, $b = 18.4264(10)$, $c = 25.8724(12)$ Å, $\alpha = 90$, $\beta = 99.4770(10)$, $\gamma = 90^\circ$, $V = 12328(12)$ Å³, $T = 173$ K, $Z = 4$, 37 856 reflections collected, 13 813 unique ($R_{\text{int}} = 0.0676$), $R1 = 0.0521$, $wR2 = 0.1338$, using 7094 reflections with $I > 2\sigma(I)$. The asymmetric unit consists of half a Mn_8 cluster and a disordered CH_2Cl_2 molecule.^[4b]
- [7] Crystal structure data for $3 \cdot 16\text{MeCN}$: $\text{C}_{136}\text{H}_{252}\text{Mn}_{16}\text{N}_{28}\text{O}_{68}$, $M_r = 4246.7$, triclinic, space group $P\bar{1}$, $a = 20.2034(17)$, $b = 21.6675(18)$, $c = 24.124(2)$ Å, $\alpha = 105.025(2)$, $\beta = 100.393(2)$, $\gamma = 104.126(2)^\circ$, $V = 9550.6(14)$ Å³, $T = 173$ K, $Z = 2$, 85 365 reflections collected, 42 222 unique ($R_{\text{int}} = 0.0531$), $R1 = 0.0468$, $wR2 = 0.1089$, using 22 696 reflections with $I > 2\sigma(I)$. The asymmetric unit consists of a Mn_{16} and 16 MeCN molecules.^[4b]
- [8] a) C. Cadiou, M. Murrie, C. Paulsen, V. Villar, W. Wernsdorfer, R. E. P. Winpenny, *Chem. Commun.* **2001**, 2666; b) L. Jones, A. Batsanov, E. Brechin, D. Collison, M. Helliwell, T. Mallah, E. McInnes, S. Piligkos, *Angew. Chem.* **2002**, *114*, 4494; *Angew. Chem. Int. Ed.* **2002**, *41*, 4318.
- [9] L. Jones, A. Batsanov, E. Brechin, D. Collison, M. Helliwell, T. Mallah, E. McInnes, S. Piligkos, *Angew. Chem.* **2002**, *114*, 4494; *Angew. Chem. Int. Ed.* **2002**, *41*, 4318.
- [10] W. Wernsdorfer, *Adv. Chem. Phys.* **2001**, *118*, 99.
- [11] A. Dolbecq, F. Secheresse, *Adv. Inorg. Chem.* **2002**, *53*, 1–41.